Melting Relations of Muscovite-Granite to 35 kbar as a Model for Fusion of Metamorphosed Subducted Oceanic Sediments

W. L. Huang and P. J. Wyllie

Department of the Geophysical Sciences,
University of Chicago, Chicago, Ill., 60637, U.S.A.

Abstract. Muscovite-granite was reacted in cold-seal pressure vessels at 2 kbar and in piston-cylinder apparatus between 10 and 35 kbar, with just 0.6 weight per cent water structurally bound in 14 modal per cent muscovite, and with additional water contents varying to 50 weight per cent. Phase relationships are presented through the melting interval with excess water, and with no free water added. Selected reactions above 10 kbars have been successfully reversed. An isobar at 15 kbar shows the effect of varying water contents on the mineral phase boundaries for vapor-present and vapor-absent conditions. For the dry rock, temperatures for the solidus and liquidus (quartz-out) curves, respectively, are 10 kbar—760°C, 1160°C; 15 kbar—810°C, 1220°C; 25 kbar—880°C; 1340°C; 35 kbar—1040°C, 1460°C. The solidus curve corresponds to the melting of muscovite + quartz. With water vapor present, the solidus is considerably lower, 15 kbar—610°C, 25 kbar—665°C. Water solubility in the liquid at 15 kbar is 24 ± 3 weight per cent. Maximum temperatures for quartz and feldspars in the vapor-absent region decrease considerably with increasing water content. Temperatures for the quartz-out curve at 15 kbars are 0.6% H_2O—1230°C; 24% H_2O—760°C. At 15 kbars for low water contents, water-undersaturated liquid coexists with quartz and feldspars through hundreds of degrees. Subducted pelagic sediments which metamorphosed to muscovite-bearing quartzo-feldspathic rocks would undergo two episodes of melting, beginning at different depths: (1) the first liquid dissolves all pore fluid, and transports it away when it escapes from the crystalline host, (2) reaction of muscovite yields a second liquid, with less dissolved water. According to two published thermal models for a lithosphere slab dipping at 45°, the depths would be (a) 60 km and 92 km, or (b) 17 km and 21 km. Magmas generated by partial fusion in subducted oceanic crust are cooler than the overlying crustal layers and the mantle above the slab by as much as 200°C to 300°C. This must lead to intrusion of relatively cool magma into hot rock. Consequent heating of the magma increases its prospects of reaching high levels in the upper mantle or crust before it solidifies by crossing the solidus curve.

Introduction

Plate tectonics, with its concept of consuming plate margins, has added new dimensions to the problem of the origin of intermediate and acid calc-alkaline magmas of island arcs and continental margins. Given sinking lithosphere slabs in subduction zones, many petrologists proposed that the plutonic and volcanic rocks derive from magmas generated by the progressive partial fusion of siliceous sediments and oceanic crust along the upper boundaries of the slabs (T. H. Green and Ringwood, 1968; Hamilton, 1969; Matsumoto, 1968; Oxburgh and Turcotte, 1970; Dickinson, 1970; Gilluly, 1971). These and other proposals have been reviewed in several recent papers including those by Boettcher (1973), Brown (1973), Fyfe (1973), D. H. Green (1972, 1973), Kushiro (1973) and Wyllie (1973).

Mantle peridotite above or below the subducted oceanic crust, as well as the deep continental crust, may also be involved in the magmatic processes. The extent of involvement of these various materials should eventually be deciphered by isotope and trace element studies of appropriate rocks but, at present, interpretation of available data does not give consistent solutions (Armstrong, 1968, 1971; Tatsumoto, 1969; Armstrong and Cooper, 1971; Oversby, 1972; Church, 1973; Church and Tilton, 1973; Faure and Powell, 1972; Doe, 1970; Donnelley and others, 1971; H. P. Taylor, 1968; S. R. Taylor, 1969; S. R. Taylor, Capp and others, 1969; S. R. Taylor, Kaye and others, 1969; Jakeš and Gill, 1970; Jakeš and White, 1970, 1972; Gill, 1970).

Another way to evaluate proposed processes is by comparison of the experimentally determined melting relationships of the observed products of magmatic activity, the calc-alkaline plutonic and volcanic igneous rock series, with the melting relations of the inferred source materials, mantle peridotite and the oceanic crust including sediments, through the pressure range extending from the surface to the deep sources. For crustal pressures, Robertson and Wyllie (1971 b) reviewed experimental results with excess water, and water-deficient conditions were considered by Burnham (1967), Brown and Fyfe (1970), and Robertson and Wyllie (1971 a). Additional experimental studies with calc-alkaline rocks at crustal pressures include those of Holloway and Burnham (1972) and Eggler (1972).

Many of the relevant experimental studies at mantle pressures are discussed in the reviews cited above. T. H. Green and Ringwood (1968) studied the melting relationships of the calc-alkaline series basalt-andesite-rhyolite, dry; T. H. Green (1972) and Stern and Wyllie (1973 a) studied them with varying water contents; Allen and others (1972) studied near-liquidus relations of basalt and andesite with excess water and oxygen buffers, with particular attention paid to amphibole stability; Stern and Wyllie (1973 b) outlined the water-saturated and water-undersaturated crystallization interval of rhyolite, using a granite composition, up to 35 kbars pressure.

The melting of hydrous minerals may play an important role for magma generation both in the crust and mantle (Yoder and Kushiro, 1969; Brown and Fyfe, 1970; Robertson and Wyllie, 1971 a; Modreski and Boettcher 1972, 1973) so here we extend the rhyolite results with detailed phase diagrams for a muscovite-granite (Huang and Wyllie, 1973 a). The dehydration and melting of muscovite-bearing rocks supplies water and potassium for pore fluids and magmas.

The starting material is similar to many granitic plutonic rocks of the crust, and it may also be considered to represent at least the low-melting portion of some subducted oceanic sediments with composition capable of metamorphism to muscovite-bearing quartzo-feldspathic rocks. For comparison, we have also studied melting reactions for assemblages of muscovite, sanidine, and quartz in the system K_2O—Al_2O_3—SiO_2—H_2O (Huang and Wyllie, 1973 b, manuscript in preparation).

The crushed rock sample from the Harney Peak Granite North Dakota, was kindly supplied by Drs. J. J. Norton and R. T. McLaughlin, U.S. Geological Survey. Table 1 gives its chemical analysis and norm. The rock contains 13.8 wt% muscovite, 80.5 wt% quartz + feldspar, 0.1 wt% biotite and 0.9 accessory minerals (garnet + opaque minerals + apatite). (McLaughlin, 1971, personal communication). Electron microprobe analysis revealed 6.7 mol% of

paragonite dissolved in the muscovite, 5.1 mol % of anorthite in plagioclase, and 6.4 % of albite in orthoclase.

Powdered rock sample (average grain size 40-60 microns) with selected water content or with no added water was sealed in a platinum capsule and reacted in a piston-cylinder apparatus with a half inch diameter piston. The piston-out procedure was used, and nominal pressures are reported, with no correction for friction. Experiments at 2 kbar pressure were conducted in cold-seal vessels.

Melting Interval of Muscovite-Granite with Excess Water

Fig. 1 shows the P-T projection for the melting interval of the muscovite-granite with excess water, between 25 and 50 weight per cent. The solidus is identical within the limits of experimental error with that for the biotite-granite studied by Stern and Wyllie (1973b; also Boettcher and Wyllie, 1968a), as well as the melting curve for the eutectic and liquidus minimum in the system $NaAlSi_3O_8$—$KAlSi_3O_8$—SiO_2—H_2O (Merrill, Robertson and Wyllie, 1970; Huang and Wyllie, unpublished).

The subsolidus assemblage at crustal pressures with excess water corresponds to that of the natural rock, two feldspars, quartz, and muscovite, with just a trace of garnet. At high pressures this becomes jadeite + coesite + muscovite + vapor. The change is caused by the breakdown of plagioclase to yield jadeite plus quartz at about 17 kbars (Boettcher and Wyllie, 1968b), which is also responsible for the change in slope of the solidus (Boettcher and Wyllie, 1978a); by the transition of quartz to coesite at about 27 kbars (Kitahara and Kennedy, 1964); and by the disappearance of orthoclase at about 22 kbars, which other evidence (Stern and Wyllie, unpublished) indicates is due to solution in the excess vapor, as speculated by Boettcher and Wyllie (1968a). The traces of accessory garnet were not observed in runs at pressures of 20 kbars or above, nor in runs at temperatures more than 25°C above the solidus.

Quartz or coesite was the liquidus phase for the granite studied by Stern and Wyllie (1973b), and the corresponding boundary is shown by the heavy line in Fig. 1. For our aluminous granite, traces of corundum or kyanite persisted to temperatures above this boundary. These minerals were produced from muscovite at temperatures near its upper stability boundary.

At 10 and 30 kbars the muscovite out curve is at 25°C and 40°C, respectively, below the melting curve for muscovite + quartz with excess water (Huang and Wyllie, 1973b, 1973c, manuscript in preparation) which is consistent with the composition of the natural mica. At 2 kbars, however the mica persisted to temperatures about 50° C higher than the maximum stability temperature of muscovite in the presence of quartz. We attribute this to incomplete reaction at 2 kbars, because reaction rates in granitic systems are notoriously slow (Piwinskii, 1967). Water at pressures greater than 10 kbars, however, has a remarkable kinetic on silicate reactions (Newton and Goldsmith, 1973), and Piwinskii and Martin (1970) have demonstrated this for granite water systems at 10 kbars. We reversed the liquidus boundaries within 25°C brackets for quartz and kyanite, respectively, at 15 and 25 kbars, and we are therefore confident that most of the phase boundaries at 10 kbars and above represent equilibrium; the only nonequilibrium feature is the appearance of traces of corundum from the breakdown
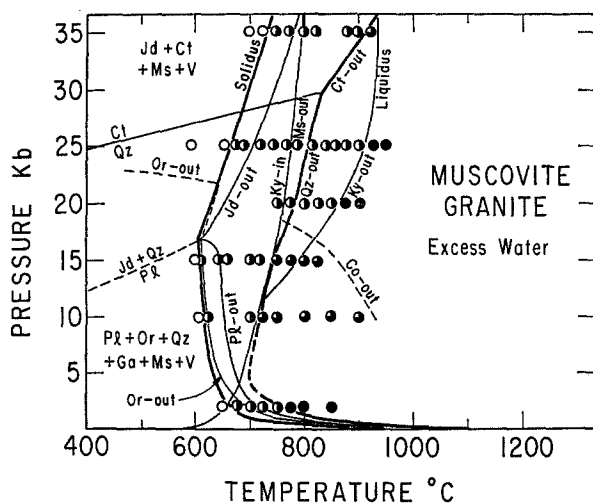
Fig. 1. Experimentally determined pressure-temperature projection for the melting interval of muscovite-granite in the presence of excess water. Abbreviations: *Pl* plagioclase; *Or* orthoclase; *Qz* quartz; *Ga* garnet; *Ms* muscovite; *Jd* jadeite; *Ky* kyanite; *Co* corundum; *Ct* coesite; *V* vapor phase

Table 1. Chemical and Normative Composition of Muscovite-Granite (L26) used in the Experiments

Chemical Composition

SiO_2	74.66	Quartz	37.16
TiO_2	0.03	Orthoclase	18.20
Al_2O_3	15.55	Albite	36.28
Fe_2O_3	0.17	Anorthite	0.98
FeO	0.42	Corundum	4.80
MnO	0.07	Magnetite	0.25
MgO	0.02	Ilmenite	0.06
CaO	0.42	Apatite	0.36
Na_2O	4.29	Calcite	0.05
K_2O	3.08	Water	0.70
H_2O^+	0.66		
H_2O^-	0.04	Total	99.59
P_2O_5	0.15		
F	0.04		
CO_2	0.02		
	99.62		
$O \equiv F$	—0.02		
Total	99.60		

J. C. DeVine and J. B. Bodkin Analysts.
J. J. Norton and R. T. McLaughlin, U. S. Geological Survey supplied the rock.

of muscovite at 10 and 15 kbars, instead of the anticipated Al_2SiO_5 polymorph. Corundum, once formed metastably, persists indefinitely in this granite system, as well as in the synthetic muscovite systems (Huang and Wyllie, 1973c, manuscript in preparation).

The main features of this phase diagram correspond to those outlined by Stern and Wyllie (1973b), with the addition of the muscovite-out curve and fields for kyanite and metastable corundum. The increasing width of the melting interval above 5 kbar pressure, caused by the increasing temperature of the quartz-out curve, is consistent with phase relations in the synthetic Granite System, $NaAlSi_3O_8$—$KAlSi_3O_8$—SiO_2 (Luth, Jahns, and Tuttle, 1964). The composition of the liquid produced near the solidus in Fig. 1 is progressively depleted in normative quartz with increasing pressure, at least to 16 kbars, and probably to higher pressures. The disappearance of subsolidus orthoclase by solution above 22 kbars indicates that the subsolidus vapor phase is far removed from pure water in composition. When melting begins, it is possible that the orthoclase constituents dissolved in the vapor are partitioned into the liquid phase, just as crystalline orthoclase dissolves in the liquid just above the solidus at lower pressures.

Melting of Muscovite Granite with No Water Added

Only reactions near the solidus in Fig. 1 can be considered as directly applicable to problems of magma genesis because of the high water content required to saturate the liquids and thus to approach the illustrated near-liquidus relationships (Fig. 3; Stern and Wyllie, 1973b). Therefore, we have studied in addition the melting relationships of the dry granite, containing only the 0.6 weight per cent water structurally bound in the muscovite, with the results shown in Fig. 2. This is a Type II system according to the classification of Robertson and Wyllie (1971a).

The subsolidus assemblage below the jadeite reaction boundary is the same as in Fig. 1, but with vapor absent. With increasing pressure, plagioclase disappears and quartz is replaced by coesite. Alkali feldspar remains stable to high pressures in the absence of vapor. Garnet is present only in trace amounts.

Melting begins where muscovite reaction begins, releasing water for solution in a small amount of H_2O-undersaturated liquid. The mica dissolves completely in the liquid within 20°C above the solidus, and the melting curve of synthetic muscovite + quartz with no vapor is about 25°C higher (Huang and Wyllie, 1973c; manuscript in preparation). This is considerably higher than the muscovite-out curve of Fig. 1, in the presence of vapor; see the muscovite phase boundary in Fig. 3. At 2 kbars, muscovite persisted much above the stability temperature of muscovite in the presence of quartz, and again we attribute this to incomplete reaction at these low pressures in the nearly dry system.

The dashed line is a solidus between 3 and 10 kbars, presented by Brown and Fyfe (1970) for a granite with 10 and 50 % muscovite added to it; the muscovite is slightly more sodic than that in our rock. This agrees well with our determined solidus.

At 35 kbars, no liquid could be detected in runs up to about 100°C higher than the muscovite-out curve, indicating that the water released from the muscovite

Fig. 2. Experimentally determined pressure-temperature section for the melting interval of dry muscovite granite. The dashed line is the solidus for a similar rock reported by Brown and Fyfe (1970). The 2 kbar runs indicated by square symbols are with excess water. Abbreviations in addition to Fig. 1: *Fsp* alkali feldspar; *Si* sillimanite; *OrH* $KAlSi_3O_8 \cdot H_2O$; *L* liquid (glass)

Fig. 3. Isobaric diagram of the melting relations of muscovite-granite at 15 kbars with varying water contents. Triangles are runs for the dry rock, Fig. 2. Squares are other vapor-absent runs. Circles are for runs with vapor present

dehydration did not become available for the melting reaction. The reaction curve for the formation of $KAlSi_3O_8 \cdot H_2O$ (Seki and Kennedy, 1964) fits the experimentally determined solidus at 35 kbar, and although we did observe sanidine hydrate in the 35 kbar subsolidus runs, we conclude that water from the musco-

vite was incorpotared into the orthoclase. The solidus therefore follows the sanidine hydrate reaction curve above 32 kbar, and melting begins when this mineral releases water.

Muscovite with quartz dehydrates at 620°C at 2 kbars, so a small amount of free water should be available for melting by 675°C, the temperature of the granite solidus with excess water. We observed no liquid in runs to 725°C, however, and we attribute this to incomplete reaction.

There is no significant increase in amount of the trace of liquid formed through a melting interval of about 250°C above the solidus, until the alkali feldspar dissolves, near the Fsp-out curve. Note the distribution of kyanite and meta-stable corundum produced from the muscovite melting reaction. Attempts to reverse the liquidus boundary were unsuccessful, which is disappointing but not unexpected in these viscous liquids with low water content (Piwinskii and Martin, 1970). The liquidus is located at temperatures where there is a significant desrease in the percentage of quartz. Very small, scattered grains of quartz persist above this boundary, as well as traces of corundum; we interpret this as incomplete reaction in a sluggish system with liquid containing a maximum of only 0.6 weight per cent H_2O.

The two most obvious features of Fig. 2 that differ from the excess water results of Fig. 1 are the increase in solidus temperature by about 200°C, and the wide melting interval of about 450°C. In Fig. 1, feldspar coexists with liquid only through a restricted range of temperature and pressure; in Fig. 2, feldspar and quartz coexist with liquid through a temperature interval of about 300°C.

Melting of Muscovite-Granite under Water-Deficient Conditions

Fig. 1 and 2 show the phase relationships of muscovite-granite for two limiting experimental conditions, with excess water, and with no added water. Fig. 3 shows results at 15 kbars for the phase relationships between these two limits, with varying percentages of water added to the rock; and the results are extra-polated further towards the anhydrous rock composition. The composition of the muscovite-granite in Fig. 3 is shown by the arrow, at 0.6 weight per cent H_2O, and the run points from Fig. 2 are plotted as triangles. The excess water runs for 15 kbars in Figure 1 are runs in Figure 3 with more than 25 weight per cent H_2O. Robertson and Wyllie (1971b) presented a schematic diagram for granodiorite and partial experimental diagrams of this type for two syenites at 2 kbars; Wyllie (1971, p. 202) presented schematic diagrams for gabbro at 10 and 20 kbars; Whitney (1972) produced experimental diagrams for synthetic granitic compositions at 8 and 12 kbars, and Stern and Wyllie (1973b) presented a preliminary diagram for another granite at 25 kbars.

At low pressures, where the vapor phase composition is almost pure H_2O, the phase boundaries for excess H_2O are isothermal. At high pressures, where the vapor contains significant amounts of dissolved rock, they are not quite isothermal, although the departure may not be detectable within the limits of experimental measurement (Robertson and Wyllie, 1971a; Stern and Wyllie, 1973b; Whitney, 1972).

The vapor-saturation boundary separates the phase fields with vapor present from those with vapor absent. There are three solidus temperatures in this diagram, depending upon the amount of water present. For a dehydrated rock, with 0 per cent H_2O, the solidus is high, in the region of $1100°C$ (Stern and Wyllie, 1973b.) For a vapor-absent rock, with all water stored in muscovite, the solidus temperature is $810°C$. For a rock with more than 0.6 per cent water, and a free vapor phase, the solidus is at $605°C$. As long as $P_{H_2O} = P_{total}$ melting will begin at $605°C$ however small the amount of vapor.

In the vapor-absent region, upper stability temperatures for quartz, feldspars, and garnet decrease considerably with increasing water content. The muscovite breakdown temperature increases with decreasing water content, as anticipated from phase relationships in synthetic mica systems (Yoder and Kushiro, 1969; Modreski and Boettcher, 1972, 1973; Huang and Wyllie, 1972, 1973b or c). We reversed the phase boundary for quartz within a $25°C$ bracket at 15 kbars with 9.5% water added ,and at 25 kbars with only 3% water added, we reversed the boundary for the reaction jadeite + quartz $\rightleftharpoons$ albite. Therefore, we have no reason to doubt that Fig. 3 portrays equilibrium relationships.

For rocks containing a percent or two of free water, melting begins at a low temperature, but the water is completely dissolved in the liquid within a few degrees of the solidus. Continued melting proceeds through a wide temperature interval, and the H_2O-undersaturated liquid coexists with feldspar and quartz through hundreds of degrees. The liquid composition, not yet determined, is certainly deficient in normative quartz compared with the original granite (Stern and Wyllie, 1973b).

The vapor-absent muscovite-granite melts at a higher temperature to yield H_2O-undersaturated liquid directly.

Fig. 3 also confirms that during crystallization of a granitic liquid containing any reasonable initial water content (and no other dissolved volatile component), the separation of a free vapor phase occurs at a very late stage in the crystallization process (Jahns and Burnham, 1969; Robertson and Wyllie, 1971a). Also, feldspars coexist with liquid through a wide temperature interval for a considerable range of water contents, giving plenty of opportunity for development of the complex zoning so characteristic of many feldspars in both plutonic and volcanic rocks.

The solubility of H_2O in this granite liquid at 15 kbars pressure, estimated by the intersection of the liquidus with the vapor-saturation boundary in Fig. 3, is between 20 and 25 weight per cent. This is the same interval reported for another granite at 25 kbars by Stern and Wyllie (1973b).

Anatexis of Metamorphosed Sediments in Subduction Zones

Processes of magma generation associated with subduction zones are undoubtedly complex (D. H. Green, 1972; Boettcher, 1973, Wyllie, 1973). Before we can begin to quantify specific models we must know three things. The composition and mineralogy of the rocks at the sources, including water content; the phase relationships of this material; and the temperature distribution in and around the subducted slab as a function of pressure, or depth. We have inferred compositions of source materials, and phase relationships are becoming available, but the variety
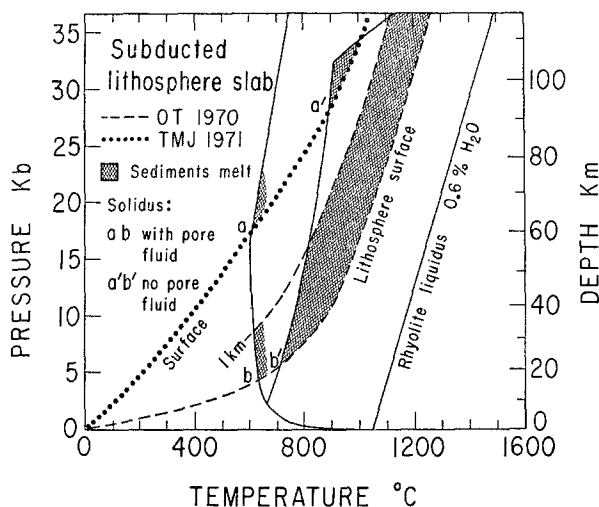
Fig. 4. A model for anatexis of a subducted oceanic sediments in pressure (depth)—temperature projection showing two episodes of melting. The curves *b-a* and *b'-a'* are the solidus curves from Fig. 1 and 2, respectively. The dashed curves indicate published estimates of temperature distributions along the surface, and 1 km below the surface of a subducted lithosphere slab, according to Oxburgh and Turcotte (1970). The dotted curve indicates another estimate along the surface of a subducted lithosphere slab published by Toksöz, Minear and Julian (1971). See text for details

of thermal models published indicates that temperature as a function of pressure is inadequately known. Eventually, the results of experimental petrology will place constraints on the thermal models (Wyllie, 1973).

Oxburgh and Turcotte (1970) outlined a model for magma generation with a zone of partial fusion that "gradually eats into the sinking lithosphere as its temperature rises and as the lowest melting fractions are removed". The first liquids are produced from metamorphosed sediments, and at greater depths the oceanic crust is fused. They calculated temperature/pressure paths for parts of the sinking lithosphere slab (45°C dip) at depths of 0 km (its surface), and 1, 2, and 5 km below its surface. The paths for the surface and 1 km depth are reproduced as the dashed curves in Fig. 4. Fitton (1971) explored the model for the oceanic crust, combining these paths with the gabbro-water phase diagram of Lambert and Wyllie (1968; see also 1972). In Figure 4, we use the results from Figures 1 and 2 to explore the progressive melting of sediments that may be carried down in a subduction zone with a dip of 45°.

Fig. 4 compares the temperature/pressure paths calculated by Oxburgh and Turcotte (1970) with a temperature/pressure path for the subducted lithosphere surface (0 km) calculated by Toksöz, Minear, and Julian (1971, Fig. 7). At various depths in the upper mantle between 40 and 120 km below the earth's surface, estimated temperatures for the surface of the lithosphere slab differ by 250–500°C. This gives some indication of the uncertainty in thermal models (Wyllie, 1973).

The metamorphism of many pelagic or ocean trench sediments could produce a rock composed dominantly of mica, quartz, and two feldspars (Garrells and

Mackenzie, 1971, Chapter 8). We therefore use the phase diagrams in Figs. 1, 2, and 3 as guides for the melting behavior of subducted sediments. The solidus curves from Figs. 1 and 2 are reproduced in Fig. 4 as lines a-b and a'-b', respectively. These two curves show the conditions for two episodes of melting in subducted sediments, the first involving interstitial aqueous pore fluid trapped within the sediment, and the second involving muscovite-bearing sediment with all free water removed. The rhyolite liquidus with 0.6 % H_2O is from Fig. 2; it shows the temperature required to produce a rhyolite liquid if only 0.6 % H_2O is available.

Consider subduction of sediment according to the thermal model of Toksöz, Minear and Julian (1971), with a lithosphere slab dipping at 45°. The temperature at the surface of the lithosphere slab then increases along the dotted line a-a' in Fig. 4. If interstitial aqueous pore fluid is trapped within the sediment, melting begins at point a, at a depth of about 60 kms. The first liquid is saturated with H_2O, but all of the pore fluid dissolves in a narrow temperature interval, and with progressive fusion the liquid becomes H_2O-undersaturated (see Fig. 3).

With continued sinking of the slab, deeper levels of the sediment layer begin to melt, as shown by the shaded area extending from a. Melting continues as the sediment layers are carried deeper below the earth's surface, producing an inclined fusion zone extending down through the sediment layer. A stage would probably be reached when sufficient magma is produced for this to become squeezed out of the slab into the overlying mantle, carrying the dissolved pore fluid with it. The remaining dry sediment would then move downwards with no further fusion until it reached the second solidus curve, b'-a', at point a' at 92 km depth, where the muscovite participates in a melting reaction. The second melting zone is shown by the shaded area extending from a'.

According to the thermal model of Oxburgh and Turcotte (1970), the two episodes of melting begin at much shallower depths, at points b and b', respectively, where the surface of the slab reaches depths of 17 and 21 kms. The shaded band extending from b represents the inclined fusion zone through a sediment layer with thickness 1 km. Melting begins at the base of this layer at a depth of about 32 kms.

This is a hypothetical model for illustrative purposes only. If oceanic sediment is dragged downwards into the mantle in a subduction zone, it is most unlikely that it would be present as a continuous layer 1 km thick. A more realistic model might involve thinner, isolated pods or blocks of sediment bounded by the faults that must have developed as the horizontal slab dipped into an inclined subduction zone.

If we assume that this first batch of magma escapes from the sediment into the overlying mantle, there is an interval with no fusion until the second episode of melting begins at point b', at the top of the sediment layer. This fusion zone extends through the sediment layer, reaching its base at a depth of about 55 km, and the complete 1 km-thick sediment layer undergoes progressive fusion as it is transported deeper. If the magma does not escape, the progressive fusion zone could continue to deep levels, as indicated by the long shaded zone in Fig. 4. If the magma escapes, carrying its dissolved water with it, the remaining anhydrous sediment yields no additional liquid in Fig. 4; further melting would require that the temperature reaches the dry solidus for the rock, which would probably exceed 1300° C at a depth of 100 km (Stern and Wyllie, 1973 b).

The two episodes of melting according to this thermal model are so close together, that they could overlap. Consider the shaded fusion zone extending from point b. If the magma did not escape from the enclosing sediment, this zone would overlap b' and become continuous with the shaded fusion zone extending from b'.

Fig. 4 illustrates some interesting features of magma generation in a subducted, hydrated oceanic crust. Assume that the two shaded fusion zones remain distinct, and consider the sediment layer as it melts at a depth of 34 kms. Magma is generated simultaneously near the base of the layer at temperatures near 630–650°C, and also in the upper half of the layer, at temperatures rising from 750°C in the center 850°C at the surface of the subducted slab. The magma from the lower part of the sediment layer escapes from its crystalline host and rises through the partially melted upper layers, where it could mix with the interstitial magma present there.

If the 640°C magma generated at the base of the sediment layer at a depth of 34 km rises through 2 km to a depth of 32 km, it passes right through the sediment layer and into the overlying mantle, where the temperature exceeds 850°C. A cool magma emplaced into a hotter rock is an unusual situation. If the magma rises slowly enough to reach thermal equilibrium with its surroundings, its temperature/pressure path on Fig. 4 takes it well above the solidus curve b-a, giving it the capability of rising to very high levels in the upper mantle or crust before crystallization is caused by crossing the solidus.

Similarly, magma produced by partial fusion of amphibolite in the oceanic crust below the 1 km pressure-temperature path may rise and mix with interstitial magma in the overlying sediment layer. Partial fusion of amphibolite without pore fluid would occur in the depth range 60–80 km according to the thermal model of Oxbrugh and Turcotte (1970) and the phase diagram of Lambert and Wyllie (1972; see Fitton, 1971). The rising magma generated in the temperature range 700°C to 850°C would reach an environment with temperature about 1000°C at the surface of the subducted slab.

These very simple models indicate that the real processes of magma generation in a subducted oceanic crust and the overlying mantle must be complex (see Green, 1972).

References

Allen, J. C., Modreski, P. J., Haygood, C., Boettcher, A. L.: The role of water in the mantle of the earth: The stability of amphiboles and micas. Proc. 24th Int. Geol. Congr. **2**, 231–240 (1972)

Armstrong, R. L.: A model for the evolution of strontium and lead isotope in a dynamic earth. Rev. Geophys. **6**, 175–199 (1968)

Armstrong, R. L.: Isotopic and chemical constraints on models of magma genesis in volcanic arcs. Earth Planet. Sci. Lett. **12**, 137–144 (1971)

Armstrong, R. L., Cooper, J. A.: Lead isotopes in island arcs. Bull. Volcanol. **35**, 27–63 (1971)

Boettcher, A. L.: Volcanism and orogenic belts—the origin of andesites. In: P. J. Wyllie ed., Experimental petrology and global tectonics. Tectonophysics **17**, 223–240 (1973)

Boettcher, A. L., Wyllie, P. J.: Melting of granite with excess water to 30 kilobars pressures. J. Geol. **76**, 235–244 (1968a)

Boettcher, A. C., Wyllie, P. J.: Jadeite stability measured in the presence of silicate liquids in the system $NaAlSiO_4$-SiO_2-H_2O. Geochim. Cosmochim. Acta 32, 999–1012 (1968b)

Brown, G. C.: Evolution of granite magmas at destructive plate margins. Nature 241, 26–28 (1973)

Brown, G. C., Fyfe, W. S.: The production of granitic melts during ultrametamorpism. Contr. Mineral. and Petrol. 28, 310–318 (1970)

Burnham, C. W.: Hydrothermal fluids at the magmatic stage. In: H. L. Barnes, ed., Geochemistry of hydrothermal ore deposits, p. 34–76. New York: Holt, Rinehart & Winston. Inc. 1967

Church, S. E.: Limits of sediments involvement in the genesis of orogenic volcanic rocks. Contr. Mineral. and Petrol. 39, 19–32 (1973)

Church, S. E., Tilton, G. R.: Lead and strontium isotopic studies in the Cascade mountains: Bearing on andesite genesis. Bull. Geol. Soc. Am. 84, 431–454 (1973)

Dickinson, W. R.: Relation of andesites, granite, and derivative sandstones to arc-trench tectonics. Rev. Geophys. Space Phys. 8, 813–860 (1970)

Doe, B. R.: Lead isotopes, 137 pp. Berlin-Heidelberg-New York: Springer

Donnelley, T. W., Rogers, J. J. W., Pushkar, P., Armstrong, R. L.: Chemival evolution of the igneous rocks of the Eastern West Indies: An investigation of thorium, uranium, and potassium distributions, and lead and strontium isotopic ratios. Mem. Geol. Soc. Am. 130, 181–224 (1971)

Eggler, D. H.: Water-saturated and undersaturated melting relations in a Paricutin andesite and an estimate of water content in the natural magma. Contr. Mineral. and Petrol. 34, 261–271 (1972)

Faure, G., Powell, J. L.: Strontium isotope geology 188 pp. Berlin-Heidelberg-New York: Springer 1972

Fitton, J. G.: The generation of magma in island arcs. Earth Planet. Sci. Lett. 11, 63–67 (1971)

Fyfe, W. S.: The generation of batholiths. In: P. J. Wyllie ed., Experimental petrology and new global tectonics. Tectonophysics 17, 273–283 (1973)

Garrells, R. M., Mackenzie, F. T.: Evolution of sedimentary rocks. New York: Norton Co. Inc., 1971

Gill, J. B.: Geochemistry of Viti Levu, Fiji and its evolution as an island arc. Contr. Mineral. and Petrol. 27, 179–203 1970

Gilluly, J.: Plate tectonics and magmatic evolution. Bull. Geol. Soc. Am. 82, 2383–2396 (1971)

Green, D. H.: Magmatic activity as the major process in the chemical evolution of the earth's crust and mantle. Tectonophysics 13, 47–71 (1972)

Green, D. H.: Contrasted melting relations in a pyrolite upper mantle under mid-oceanic ridge, stable crust and island arc environments. In: P. J. Wyllie, ed., Experimental petrology and global tectonics. Tectonophysics 17, 285–297 (1973)

Green, T. H.: Crystallization of calc-alkaline andesite under controlled high-pressure hydrous conditions. Contr. Mineral. and Petrol. 34, 150–166 (1972)

Green, T. H., Ringwood, A. E.: Genesis of the calc-alkaline igneous rock suite. Contr. Mineral. and Petrol. 18, 105–162 (1968)

Hamilton, W.: Mesozoic California and under flow of Pacific mantle. Bull. Geol. Soc. Am. 80, 2409–2430 (1969)

Holloway, J. R., Burnham, C. W.: Melting relations of basalt with equilibrium water pressure less than total pressure. J. Petr. 13, 1–29 (1972)

Huang, W. L., Wyllie, P. J.: Melting of muscovite to 30 kbars in the system $KAlSi_3O_8$-Al_2O_3-SiO_2-H_2O (Abstract). Trans. Am. Geophys. Union 53, (4), 552 (1972)

Huang, W. L., Wyllie, P. J.: Melting relations of muscovite-granite, with application to anatexis in the crust and subduction zones (Abstract). Trans. Am. Geophys. Union 54, (4) 481 (1973a)

Huang, W. L., Wyllie, P. J.: Muscovite dehydration and melting in deep crust and subducted oceanic sediments. Earth Planet. Sci. Lett. 18, 133–136 (1973b)

Jahns, R. H., Burnham, C. W.: Experimental studiea of pegmatite genesis: I. A model for the derivation and crystallization of granitic pegmatites. Econ. Geol. 64, 843–864 (1069)

Jakeš, P., Gill, J. B.: Rare earth elements and the island arc tholeiitic series, Earth Planet. Sci. Lett. 9, 17–28 (1970)

Jakeš, P., White, A. J. R.: K/Rb ratios of rocks from island arcs. Geochim. Cosmochim. Acta **34**, 849–856 (1970)

Jakeš, P., White, A. J. R.: Major and trace elements abundance in volcanic rocks of orogenic arcs. Bull. Geol. Soc. Am. **83**, 29–40 (1972)

Kitahara, S., Kennedy, G. C.: The quartz-coesite transition. J. Geophys. Res. **69**, 5395–5400 (1964)

Kushiro, I.: Origin of some magmas in oceanic and circum-oceanic regions. In: P. J. Wyllie ed., Experimental petrology and global tectonics. Tectonophysics **17**, 211–222 (1973)

Lambert, I. B., Wyllie, P. J.: Stability of hornblende and a model for the low velocity zone. Nature **219**, 1240–1241 (1968)

Lambert, I. B., Wyllie, P. J.: Melting of gabbro (quartz eclogite) with excess water to 35 kilobars, with geological applications. I. Geol. **80**, 693–708 (1972)

Luth, W. C., Jahns, R. H., Tuttle, O. F.: The granite system at pressure of 4 to 10 kilobars. J. Geophys. Res. **69**, 759–773 (1964)

Matsumoto, I. A.: A hypothesis on the origin of the late mesozoic volcanic-plutonic association in East Asia. Pacific Geol. **1**, 77 (1968)

Merrill, R. B., Robertson, J. K., Wyllie, P. J.: Melting reactions in the system $NaAlSi_3O_8$-$KAlSi_3O_8$-SiO_2-H_2O to 20 kilobars compared with results for other feldspar-quartz-H_2O and rock-H_2O systems. J. Geol. **78**, 558–569 (1970)

Modresky, P. J., Boettcher, A. L.: The stability of phlogopite and enstatite at high pressures: A model for mica in the interior of the earth. Am. J. Sci. **272**, 852–869 (1972)

Modreski, P. J., Boettcher, A. L.: Phase relationships of phlogopite in the system K_2O-MgO-CaO-Al_2O_3-SiO_2-H_2O to 35 kilobars: A better model for micas in the interior of the earth. Am. J. Sci. **273**, 385–414 (1973)

Newton, R. C., Goldsmith, J. R.: "Hydrothermal" reactions with traces of H_2O at high pressures. Trans. Am. Geophys. Union **54** (4), 482 (1973)

Oversby, V. M.: Lead isotopic compositions of Tonga-Kermadec volcanics and their petrogenetic significance. Contr. Mineral. and Petrol. **37**, 181–210 (1972)

Oxburgh, E. R., Turcotte, D. L.: Thermal structure of island arcs. Bull. Geol. Soc. Am. **81**, 1665–1688 (1970)

Piwinskii, A. J.: The attainment of equilibrium in hydrothermal experiments with "granitic rocks". Earth Planet. Sci. Lett. **2**, 161–162 (1967)

Piwinskii, A. J., Martin, R. F.: An experimental study of equilibrium with granitic rocks at 10 kb. Contr. Mineral. and Petrol. **29**, 1–10 (1970)

Robertson, J. K., Wyllie, P. J.: Rock-water systems, with special reference to the water-deficient region. Am. J. Sci. **271**, 252–277 (1971a)

Robertson, J. K., Wyllie, P. J.: Experimental studies on rocks from the Deboulllie Stock, Northern Maine, including melting relations in the water-deficient environment. J. Geol. **79**, 549–571 (1971b)

Seki, Y., Kennedy, G. C.: The breakdown of potassium feldspar, $KAlSi_3O_8$, at high temperatures and high pressures. Am. Mineralogist **49**, 1688–1706 (1964)

Stern, C. R., Wyllie, P. J.: Melting relations of oceanic sediments and basalt-andesite-rhyolite-H_2O compared at 30 kb (Abstract). Trans. Am. Geophys. Union **54**, (4) 481 (1973a)

Stern, C. R,, Wyllie, P. J.: Water-saturated and undersaturated melting relations of a granite to 35 kilobars. Earth Planet. Sci. Lett. **18**, 163–167 (1973b)

Tatsumoto, M.: Lead isotopes in volcanic rocks and possible ocean-floor thrusting beneath island arcs. Earth Planet. Sci. Lett. **6**, 369–376 (1969)

Taylor, H. P.: The oxygen isotope geochemistry of igneous rocks. Contr. Mineral. and Petrol. **19**, 1–71 (1968)

Taylor, S. R.: Trace element chemistry of andesites and associated calc-alkaline rocks. Proceedings of the Andesite Conference, Bull. 65, State of Oregon, Dept. of Geol. and Mineral. Industries, 43–64 (1969)

Taylor, S. R., Capp, A. C., Graham, A. L., Blake, D. H.: Trace element abundances in andesites. Contr. Mineral. and Petrol. **23**, 1–26 (1969)

Taylor, S. R., Kaye, M., White, A. J. R., Duncan, A. R., Ewart, A.: Genetic significance of Co, Cr, Ni, Sc and V content of andesites. Geochim. Cosmochim Acta **33**, 275–286 (1969)

Toksöz, M. N., Minear, J. W., Julian, B. R.: Temperature field and geophysical effects of a downgoing slab. J. Geophys. Res. **76**, 1113–1138 (1971)

Whitney, J. A.: History of granodioritic and related magma systems: An experimental study. Unpublished Ph. D. Dissertation, Stanford University, 192 p. (1972)

Wyllie, P. J.: The dynamic earth: A textbook in geosciences, 416 pp. New York: John Wiley, 1971

Wyllie, P. J.: Experimental petrology and global tectonics—A preview. In: P. J. Wyllie ed., Experimental petrology and global tectonics. Tectonophysics **17**, 189–209 (1973)

Yoder, H. S., Kushiro, I.: Melting of a hydrous phase: phlogopite. Am. J. Sci. **267**A, 558–582 (1969)

Dr. W. L. Huang
Prof. Dr. P. J. Wyllie
Department of the Geophysical Sciences
University of Chicago
Chicago, Illinois 60637, U.S.A.